Evaluation of Broadband Decoupling Schemes for In Vivo NMR Spectroscopy

R. A. de Graaf[1], P. van Eijsden[1], P. Brown[1], S. McIntyre[1], T. Nixon[1]
[1]MRRC, Yale University, New Haven, CT, United States

Introduction

Most broadband decoupling schemes have been optimized for high-resolution, liquid-state NMR spectroscopy (see [1] for review). However, the requirements for *in vivo* NMR spectroscopy are sufficiently different to demand a re-evaluation of existing broadband decoupling schemes. The available RF power for *in vivo* NMR is often limited by inefficient coils, while the allowable RF power is determined by tissue heating boundaries. Furthermore, at the typical magnetic fields used for *in vivo* NMR the required decoupling bandwidth is relatively narrow, while the spectral resolution is often an order of magnitude lower than in high-resolution, liquid-state NMR. Here we present theoretical simulations and experimental validation of broadband decoupling schemes for *in vivo* NMR with consideration of RF power, decoupling bandwidth and RF inhomogeneities.

Methods

Simulations were performed using the product operator formalism described by Skinner and Bendall [2] for a heteronuclear two-spin-system with a scalar coupling constant of 140 Hz. The spectroscopic linewidth was 6 Hz. Decoupling efficiency was calculated as the decoupled center peak height, S_{dec}, relative to the non-decoupled peak height, S_0. All results are presented for $(S_{dec}/S_0) \geq 1.8$. *In vivo* broadband decoupling was evaluated on rat brain at 9.4 Tesla one hour following the intravenous infusion of [1,6-$^{13}C_2$]-glucose. Signal was acquired with a previously described ^{1}H-[^{13}C] NMR sequence [3] from a volume of 180 µl (TR/TE = 4000/8.5 ms, NEX = 512) with a number of different decoupling schemes.

Results

Table 1 shows decoupling bandwidths for different decoupling schemes and RF amplitudes. The popular WALTZ-16 and MLEV-16 schemes [1] perform well, even for low RF amplitudes, but the bandwidth is limited to roughly twice the RF amplitude. For more demanding applications, like ^{13}C decoupling during ^{1}H-[^{13}C]-NMR spectroscopy, wider decoupling bandwidths are required. The lesser known Fn inversion pulses ([4], n = 2 or 3) form the basis of a 20-step supercycle scheme that can achieve broadband decoupling of wider bandwidths at moderate RF amplitudes. Adiabatic RF pulses offer a wider range of parameters, like modulation functions, pulse length and frequency range that can be used to optimize their performance in broadband decoupling schemes. As an example, Table 1 shows one possible adiabatic decoupling scheme based on HS8 modulation functions that can outperform all other decoupling schemes at relatively high RF amplitudes. Note that the average power of (amplitude-modulated) adiabatic pulses is often substantially lower than the peak power. Decoupling schemes that are specifically designed to perform at low RF amplitudes, GARP and PBAR, can be outperformed by other schemes at any RF amplitude. Certain applications allow selective decoupling as an alternative to complete broadband decoupling. Figure 1 shows selective decoupling and spectral editing of all resonances (15 – 55 ppm), except [1-^{13}C]-glucose (~ 100 ppm) in a ^{1}H-[^{13}C]-NMR spectrum of rat brain one hour following intravenous [1,6-$^{13}C_2$]-glucose infusion. The exclusion of [1-^{13}C]-glucose decoupling effectively reduces the decoupling bandwidth by 50%, thereby significantly lowering the demands on the decoupling scheme without sacrificing spectral information.

Discussion

The results presented here demonstrate that no single decoupling scheme is optimal under all experimental conditions. At RF amplitudes γB_1 between 0.25 and 0.40 kHz only continuous wave irradiation achieves adequate (on-resonance) decoupling. The WALTZ-16 sequence is superior at low RF amplitudes (γB_1 ~ 0.5 kHz, applicable to human brain), while adiabatic decoupling schemes can be designed to outperform all other sequences at higher RF amplitudes (suitable for rat brain). Decoupling at intermediate RF amplitudes (γB_1 ~ 1.0 kHz) offers sufficient freedom to optimize the performance, for example, by using frequency-switched Fn or partial adiabatic pulses. Most decoupling schemes offer adequate compensation towards RF inhomogeneities, making them suitable for surface coil transmission. While broadband decoupling is desirable under most experimental conditions, certain applications can benefit from modifications as demonstrated for ^{1}H-[^{13}C]-NMR (Fig 1).

Acknowledgements

The research was supported by NIH grants RO1-EB002097, DK27121 and NS34813.

References

[1] Shaka AJ, Keeler J, Prog NMR Spectroscopy 1987; 19: 47-129
[2] Skinner TE, Bendall MR, J Magn Reson 1999; 141: 271-285
[3] de Graaf RA et al, Magn Reson Med 2003; 49: 37-46
[4] Fujiwara T, Nagayama K, J Magn Reson1988; 77: 53-63

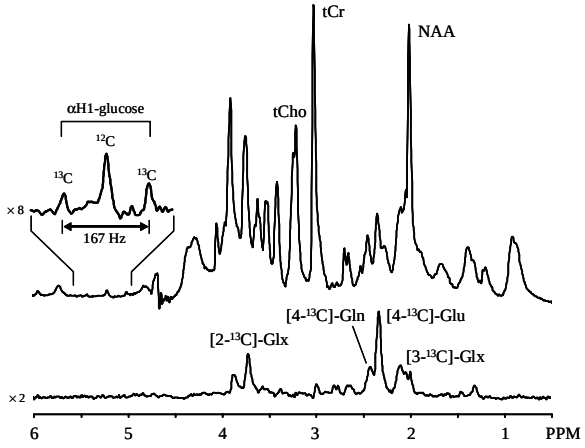

Figure 1: ^{1}H (top) and ^{1}H-[^{13}C] (bottom) NMR spectra from rat brain acquired with selective decoupling and editing. All resonances, except [1-^{13}C]-glucose are decoupled. Note the absence of [1-^{13}C]-glucose in the ^{1}H-[^{13}C]-NMR spectrum due to selective spectral editing.

Table 1 : Relative decoupling bandwidths ($\Delta\omega/\gamma B_1$) as a function of RF amplitude γB_1 for different broadband decoupling schemes.

γB_1 (kHz)	0.50	0.75	1.0	1.5
WALTZ-16	**1.64**	2.27	2.37	2.40
MLEV-16	**1.74**	2.05	2.18	2.21
F2	1.34	2.68	2.74	2.76
F3	0	**3.21**	**4.13**	**4.17**
FPI2	1.38	2.12	2.17	2.20
FPI3	1.22	2.61	2.92	3.30
GARP	0	0	1.65	**4.96**
PBAR	0.52	0.65	0.66	0.68
AFPST8	0	0	0	**5.40**
AFPTT	0	1.33	2.54	2.77